



# Evaluation of Tensile, Impact and Fatigue Crack Growth Rate of Epoxy Based Coatings used as a Lining for Crude Oil Storage Tanks

Haider Hadi Jasim

Department of Chemical Engineering, College of Engineering, University of Basrah, Basrah, Iraq, [raidhani73@yahoo.com](mailto:raidhani73@yahoo.com)

Published online: 30 June 2020

**Abstract**— Fatigue is one of the main causes of failures in petroleum storage tanks. In order to assess the safety of the tank metal and coatings, the expected fatigue failure needs to be estimated. In this paper, the tensile, impact and fatigue resistance of three types of epoxy based coatings (pure, Phenol Novolac and reinforced by glass-flake) used as lining for crude oil storage tanks were studied using experimental method and finite elements method (FEM). Both experimental test and (FEM) were conducted on uncoated and coated ASTM A537 C1 steel in case of single and double layers. The test results showed that the applied coating improves the mechanical properties and increases of fatigue crack resistance. The fatigue crack growth rate is influenced by compositions of epoxy coating and an amine-adduct cured epoxy coating reinforced with glass-flakes show more resistance to fatigue cracks compare to amine cure by Novolac or pure epoxy. Microscopic observation of fatigue tests of specimens show the crack propagations is uniform, stable and linear types.

**Keywords**- functionality, epoxy coating, fatigue cracks, J-Integral, glass-flakes.

## 1. Introduction

Fatigue and corrosion, in general, are the major cause of structural failure and occurs in various petroleum applications include pipelines and tanks. The study of crude oil storage tanks fatigue and corrosion are importance for efficient tank economics and safety [17]. The fatigue failure can be described as material structural damage due to action of cyclic stress [15]. One of the most efficient methods used to protect the crude oil storage tanks from internal corrosion by applying epoxy coatings. The tanks are usually exposed to continuous full and discharging operations by crude oils. Full of tanks and discharging operations exhibition the internal coating to stresses have a maximum value when fully filled and less valuable when discharged, resulting in the internal coating being deformed, fatigued and cracked [12, 29].

Various numerical and experimental methods were used for analyzing of fatigue of cracked structures. The finite element method FEM is a numerical technique used to obtain approximately solution of the engineering problems. The FEM has a practical application in engineering fatigue fracture analysis to evaluate the stresses, strains and displacements during cycling loading of fatigue tests [19]. The tensile and impact properties of coatings have influences on the properties of the steel material, so conducted these testing are important to determine the mechanical properties and resistance to dynamic impact loading [1]. Fatigue crack growth rate

(FGGR) testing using a compact tension specimen contains a sharp crack is conducted to determine the resistance of material to crack extension under cyclic loading conditions. The fatigue crack growth rate testing provides a relationship between various parameter effects on a crack growth and the accompanied crack growth rate. The information obtained from fatigue crack growth rate testing can be used to predict the structures safe lifetime when cracks are found [27].

Few limited studies and researches were conducted into fatigue behavior of epoxy coatings. Ringsberg et al. [18] used the finite element method to analysis and calculate the plastic strains of water ballast tanks epoxy coating applied on steel substrates under cyclic tensile strains. Their results indicated that the unaged coating type has a longer predicted life than the aged film coating and the embrittlement of coating is attributed to the ageing was considered the main reason of premature cracking in coating during service. Sadananda et al. [21] presented a review of coatings/substrates fatigue behavior and demonstrated that the fatigue damage is either general or local depending on the range of cyclic loads. The fatigue crack initiation can result from the local damage in coatings, whereas the general fatigue damage results when the loads are of longer range like cyclic bending, uniaxial and biaxial tension and compression. Fang et al. [26] studied high and low fatigue crack growth rate behavior of acrylonitrile-butadiene-styrene (ABS) and polycarbonate (PC). They discovered the crack surfaces

have rough characteristics in the higher crack growth rate, whereas at lower crack growth rate, the crack surfaces have smooth characteristics. Kanchanomai et al. [10] correlated the fatigue crack growth rates ( $da/dN$ ) of polyamine cured thermoset epoxy coating by the linear and nonlinear-elastic fracture mechanics parameters  $\Delta K$ ,  $K_{max}$  and  $\Delta J$  respectively. They showed that these parameters ( $\Delta K$ ,  $K_{max}$  and  $\Delta J$ ) are affected by a stress ratio. Andres et al. [14] studied the mechanisms of emergence and fatigue cracks growth by various mechanical tests including tension, Charpy impact, bending guided and axial fatigue of ASTM A537 and ASTM A240 structural steels. Their results indicated the microstructure and mechanical properties can be considered adequate to withstand the loading requirements during service lifetime. Xu et al. [30] established the fatigue behavior of thermoset polymeric coatings. They found that as the coating thickness increased, there are a widespread of delamination between the steel substrate and the coating layer. Kim et al. [8] investigated the damage in thin metal films due to the influence of the mechanical fatigue and identify that the nucleation of a fatigue-induced crack. As well as, the required number of cycles for nucleation of crack is decreased with increasing of the fatigue sample area. Andreas et al. [7] investigated the fatigue crack propagation resistance of Polymethylmethacrylate triblock copolymer on a cycloaliphatic amine cured bisphenol A based epoxy resin. Their results shows that add small concentrations of PMMA can enhance the resistance of epoxy coating to fatigue crack propagation rate. Wu et al. [28] studied the fatigue cracking development morphology in epoxy coatings used for marine ships. They found that the development of crack in surface is started soon after the onset of cycling and continued growth of surface channeling cracks.

The developed of cracks and resistance of epoxy coatings is effected by tensile, impact and cycling loading. So, in this paper presents a comparative study of tensile, impact and fatigue crack resistance of the three different types of epoxy coatings in case of single and double layers of coats. Fatigue crack propagation rate was measured experimentally and compared with finite element analysis using Ansys software V6.7.

## 2. Epoxy Based Coatings and Materials Tested

### 2.1 Epoxy Based Coatings

The epoxy based coating consists of two parts the base and a hardener found in the liquid state and mixed together to form a coating that spraying on the steel substrate. Four types of commercial Hample epoxy coatings are studied (one type was used as a primer undercoats). These coatings are :

- A-Hample-13201 primer undercoats, this type have urethane-modified alkyd primer and manufactured by PT-Hampel of Indonesia Co., Ltd.
- HEMPADUR-15600, consists from amine adduct cured pure epoxy coat. The coat thickness in the range 160-200  $\mu\text{m}$ . This type of coating named as model A.
- HEMPADUR-85671, consists from solvent free amine cured phenol Novolac epoxy. The coat thickness in the range 250 - 600  $\mu\text{m}$ . This type of coating named as model B.
- HEMPADUR multi-strength GF-35870 is amine adducts cured epoxy reinforced by glass-flake. The maximum thickness of this coat is 350  $\mu\text{m}$ . This type of coating named as model C.

The last three Hample coatings are produced by the Hample coating company, USA.

### 2.2 Material and Coating Applications

The study is conducted on ASTM A537 C1 carbon steel which was widely applied in constructing a crude oil storage tanks of South Iraq. The material compositions are given in Table 1, while the mechanical properties are: tensile strength  $S_u = 485$  MPa, yield strength  $S_y = 345$  MPa and modulus of elasticity  $E = 203$  MPa [25].

**Table 1:** The chemical composition of ASTM A537 carbon steel.

Elements	Wt. %
Fe	97.58
C	0.24
Mn	1.6
P	0.035
S	0.035
Cr	0.025
Si	0.5
Mo	0.8
Ni	0.25
Cu	0.35

The process of applied epoxy based coating including three steps surface preparation, cleaning the surface and then the coatings is applied. After surface preparation and clean-up process, the Hample-13201 primer is applied directly onto the steel substrate by airless spray method. The primary function of the primer was to improve the overall adhesion of subsequently applied epoxy layer. Then, the three types of epoxy coatings are applied into the steel substrate at a sufficient coating film thickness that given by the standard of company manufactured recommendation. To ensure the coating thickness in the range of uses, the coating thickness is measured using a paint thickness meter manufactured by Gain Express Holdings Ltd, China. The thickness as an average values of the single and double layers are 180  $\mu\text{m}$  and 250  $\mu\text{m}$  for model A, 300  $\mu\text{m}$  and 425  $\mu\text{m}$  for model B, 290  $\mu\text{m}$  and 325  $\mu\text{m}$  for models C.

### 3. Experimental Methods

#### 3.1 Tensile Test

A tensile test is conducted to determine the mechanical properties including tensile strength, yield strength, Poisson's ratio and modulus of elasticity. Figure 1A shows the shape and dimensions of the tensile test specimen according to ASTM E8M-01 [13]. Figure 1B to 1H show the specimens before and after applied a single and double layers of coatings. A tensile testing machine (Hounsfield tensile machine SM1002, Hounsfield Company, UK) is used to perform the test.

The tensile test involves mounting in a testing machine the coated and uncoated specimens and subjecting them to uniaxial tensile force. Tensile forces vs. elongations of the gage length are recorded during the test and then converted to stress and strain data using the following equations [22]:

$$\sigma = \frac{F}{A_o} \quad (1)$$

$$\varepsilon = \frac{\Delta L}{L_o} \quad (2)$$

Where,

F: applied tensile force in kN.

$A_o$ : the initial area of the gage part in  $m^2$ .

$L_o$ : the initial length of gage part in mm.

$\Delta L$ : change of gage length during a test in mm.

#### 3.1 Charpy Impact Test

Charpy V-notched specimens were machined from A537 C1 steel plate material with dimensions shown in Figure 2A in accordance with the ASTM E23-72 standard [2]. Figure 2 B to H show specimens before and after coatings with the three types of coatings. The test specimen is supported at its two ends and struck by the pendulum on the opposite face to the notch. The energy absorbed after the fracturing specimen is measured and it is given an indication of material toughness, resistance of material to damage and deformation. The JB-300B testing machine manufactured by Jinan-Tianchen Co., China was used for conducting the test.

#### 3.2 Fatigue Test

The standard compact tension specimen (CT) is a single-edge notched located in midsize, fabricated according to ASTM E647 [3]; the specimen geometry and dimensions in mm are shown in Figure 3A and have 12.5 mm thickness. The specimen before and after coatings by the three models of coats in case of single and double layers are shown in Figure 3B to H. Fatigue test experiments were performed on Bi-04-CP-310 universal testing machines manufactured by TCR engineering Co. Pvt., India.

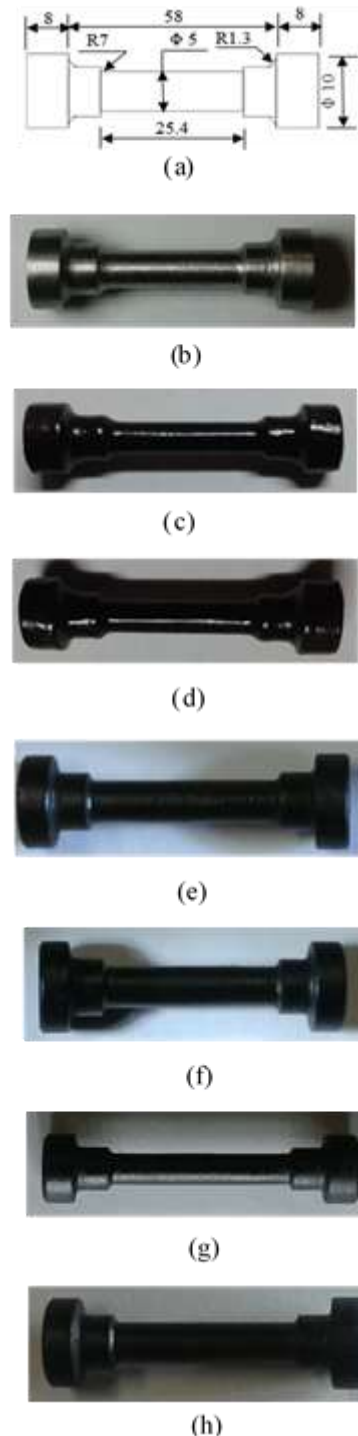


**Figure 1:** Tensile test specimen before and after coatings.

- |                          |                          |
|--------------------------|--------------------------|
| (a) Specimen dimension   | (b) Before coating       |
| (c) Single layer model A | (d) Double layer model A |
| (e) Single layer model B | (f) Double layer model B |
| (g) Single layer model C | (h) Double layer model C |

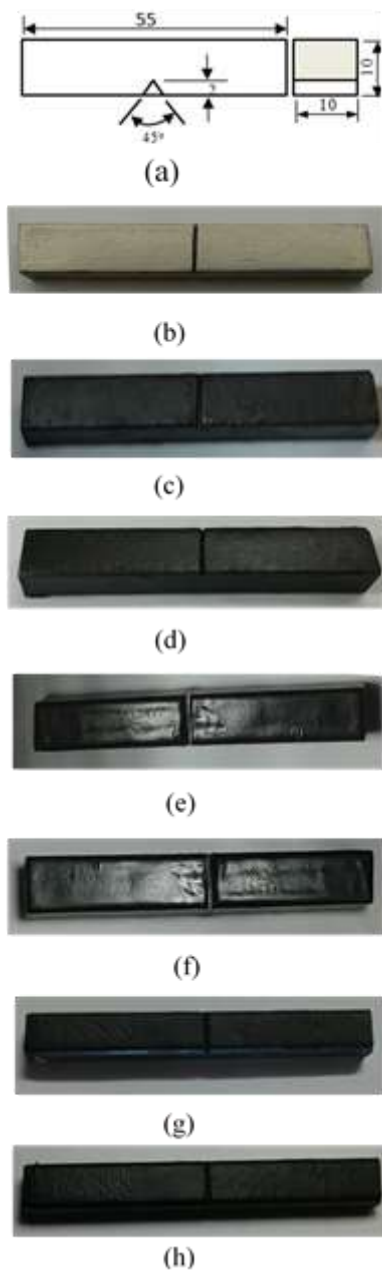


**Figure 2:** Charpy specimens before and after coatings.  
 (a) Specimen dimensions (mm) (b) Before coating  
 (c) Single layer model A (d) Double layer model A  
 (e) Single layer model B (f) Double layer model B  
 (g) Single layer model C (h) Double layer model C

The fatigue crack propagation rate is determined by subjecting CT specimen to constant amplitude cyclic loading (P). The incremental increases in crack length are recorded with the corresponding number of load cycles acquire data of crack length (a) and cycle count (N). The data is presented in (a vs. N) curve, various curves can be generated by varying the magnitude of the cyclic loading for different identical test specimens have same initial crack length  $a_0$  and are shown in Figure 4.

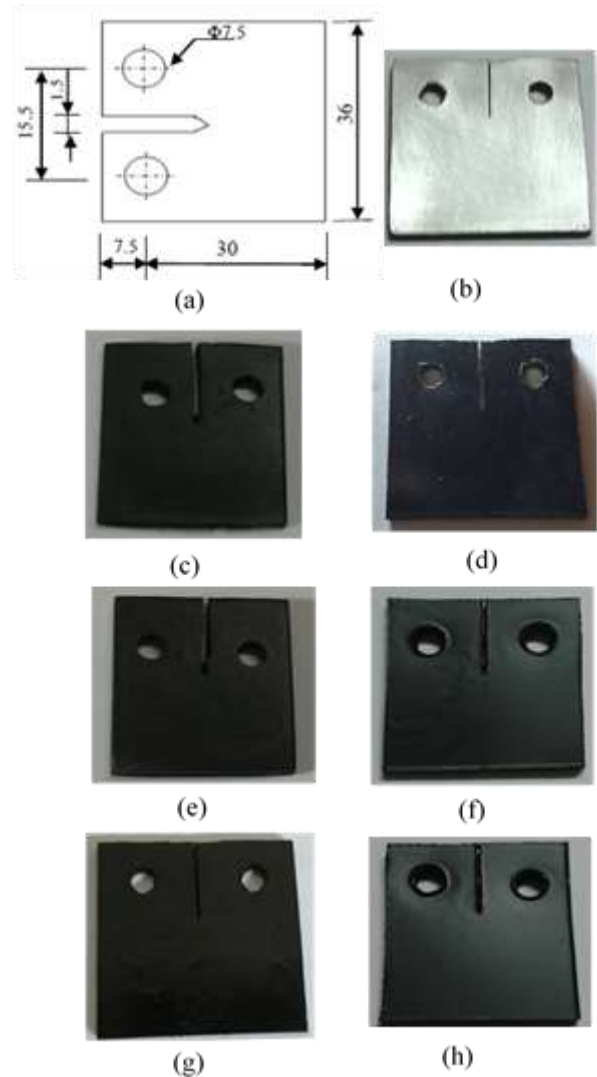


**Figure 3:** Fatigue specimens before and after coatings.  
 (a) Compact tension specimen (b) Before coating  
 (c) Single layer model A (d) Double layer model A  
 (e) Single layer model B (f) Double layer model B  
 (g) Single layer model C (h) Double layer model C

The secant technique for computing the crack growth rate is used for calculating  $da/dN$ . The method involves calculating the slope of the straight line connecting two adjacent data points according to the following equation [20]:

$$\frac{da}{dN} = \frac{\Delta a}{\Delta N} = \frac{a_{i+1} - a_i}{N_{i+1} - N_i} \quad (3)$$

Where,  
 $da/dN$ : Crack growth per load cycle mm/cycle.  
 N: Number of cycles.

The stress intensity factor at the crack tip of a compact tension specimen was calculated using the following formula [9]:

$$K = \frac{P}{B} \sqrt{\frac{\pi}{W}} [16.7 \left(\frac{a}{W}\right)^{0.5} - 104.7 \left(\frac{a}{W}\right)^{1.5} + 369.9 \left(\frac{a}{W}\right)^{2.5} - 573.8 \left(\frac{a}{W}\right)^{3.5} + 360.5 \left(\frac{a}{W}\right)^{4.5}] \quad (4)$$

Where,

a: Crack length mm.

P: Applied load kN.

B: Thickness of the specimen mm.

W: Width of the specimen mm.

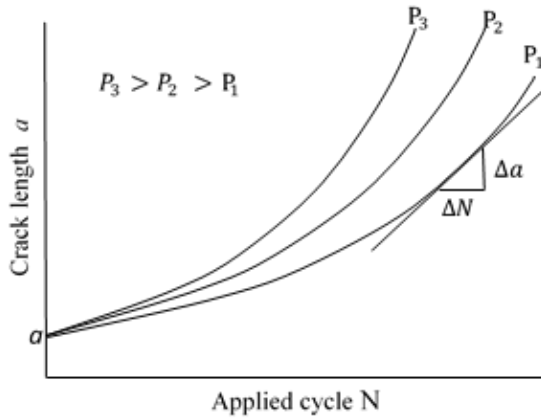


**Figure 4:** Crack length vs. applied cycles.

The load increment applied from 5 to 20 kN by increasing 0.5kN for each cycle until failure occurs. During test, the crack length is measured using microscopic having magnification of 50 times and then use Eq.(4) to calculate the stress intensity factor The fatigue crack propagation rate under constant cyclic loads described by the Paris and Erdogan relationship which is expressed as [23]:

$$\frac{da}{dN} = C (\Delta K)^m \quad (5)$$

And

$$\Delta K = K_{\max} - K_{\min} \quad (6)$$

Where,

C and m: Pares constants.

$K_{\max}$  and  $K_{\min}$ : The max. and min. values of stress-intensity factor MPa. $\sqrt{m}$ .

#### 4. Finite Element Analysis (FEM)

Finite element method (FEM) was applied to calculate the stress intensity factor in the case of an open mode (mode I) of compact tension specimen. In this paper, using special program Ansys V6.7 software in addition to the J-Integral program to calculate stress intensity factor. Use J-Integral way because its description elastic-plastic behaviors at the tip notch of material.

Because of the high crack tip constraint due to the side grooves, the compact tension specimen may be modeled in 2-D plane strain and considered as an isotropic in FEM analysis. The finite element mesh for compact tension specimen has unit thickness using 3-nodes element is shown in Figure 5.

In the Ansys V6.7 software, symmetric boundary conditions were applied. The displacement of all elements nodes of Figure 5 is constrained along the x-axis, while all nodes lie on crack length will be consider free displacement, The compact tension specimen contains a pair of holes which represents a pin, through which the loads are applied on the nodes lie on the holes of compact tension specimen along y-axis.

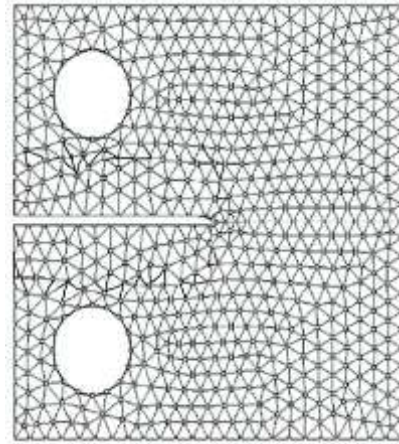


**Figure 5:** Finite element divisions using 3 nodes triangular element.

J-Integral represented the energy release rate and can be calculated by a path independent line integral [20]. For fatigue crack growth rate analysis of compact tension specimen, since during unloading condition, the integral path independency of J-Integral is not evaluated, this use the J-Integral range ( $\Delta J$ ) as the fracture parameter. The J-Integral range ( $\Delta J$ ) is computed during cyclic loading and defined as the difference between maximum and minimum values of J-Integral during loading applied. The relation between J-Integral range and stress intensity factor range during cyclic loading is as follows [4]:

$$\Delta J = \frac{(\Delta K)^2}{E} \quad (7)$$

Where,

E: Modulus of elasticity MPa.

$\Delta K$ : Stress intensity factor range MPa. $\sqrt{m}$ .

The J-integral expression for 2-D crack in mode I of linear elastic fracture mechanics is defined as [25]:

$$J = \int_{\Gamma} W_i dy - \int_{\Gamma} T^t \frac{\partial u}{\partial x} ds \quad (8)$$

Where,

J: Effective energy release rate N/mm.

$W_i$ : Strain energy density J/m<sup>3</sup>.

T: Traction vector.

ds: Differential element along the contour.

u : Displacement vector.

t: Transpose of matrix.

$\Gamma$ : Arbitrary counter clockwise contour.

x: Cartesian coordinate being parallel to the crack tip.

y: Cartesian coordinate being normal to the crack tip.

The strain energy  $W_i$  is calculated from the following formula [16]:

$$W_i = \int_0^{\underline{\varepsilon}} \underline{\sigma}^t d\underline{\varepsilon} = \frac{1}{2} \underline{\sigma}^t \underline{\varepsilon} \quad (9)$$

Where,

$\underline{\varepsilon}$  : Strain vector.

$\underline{\sigma}$ : Stress vector.

## 5. Results and Discussion

### 5.1 Tensile Test Results

The force- displacement data for ASTM A537 C1 steel in case of uncoated and coated by the three types of Hampel epoxy coats were recorded using a tensile test. Then, the data were converted to a corresponding stress-strain curves using Eq.(1) and Eq.(2) and it is shown in Figure 6. The mechanical properties (tensile strength, yield strength and modulus of elasticity) are obtained from the stress-strain curves of Figure 6. Table 2 is summarized these mechanical properties. The inflection of curves is occurred at 0.02 strains for A537 steel and 0.025 strains for all coated specimens. At this point of inflection, the cracks starts to generate as visually observed during conductive the test. The tensile stress at this point was calculated as the yield strength. The strength increases with increases of applied loading until the strain becomes 0.36 and then it is decreased until complete failure occurs. Improvements in the tensile properties of the coated specimens were attributed to that the epoxy layers improve the strength of the test specimen during tests.

Glass-flakes in model C offer various aspects of enhancement, particularly extension and compression resistance, depending on the orientation of glass-flakes within the epoxy based coats structure. It can reduce the segmental movement of the epoxy coating chains, i.e. reduce the fluidity and brittleness of epoxy based coatings. This, glass-flakes increase the cross-linking density of the epoxy coating network, leading to improve the mechanical properties of the coating compared to other coat types.

Also the improvement in tensile properties attributed to the plastic deformation of the epoxy coated specimen will enhanced and increased the toughness due to the interactions of the stresses during test [5].

### 5.2 Charpy Test Results

The epoxy based coatings can withstand some degree of impact damage that occurs within a coated tank during various operational and maintenance activities. The resistance of coatings to impact loading is important because at some damage points, the fatigue crack can be initiated immediately. The Charpy test is performed at various temperatures: 15, 25, 35, and 45°C and the test results are shown in Table 3. It has been observed from Table 3, the A537 C1 steel coated by model C provides larger values of impact energy. In addition, for all

coatings, the impact energy is increased by small values if the number of coatings layers is increased, but the significant difference at high temperatures is become very small.

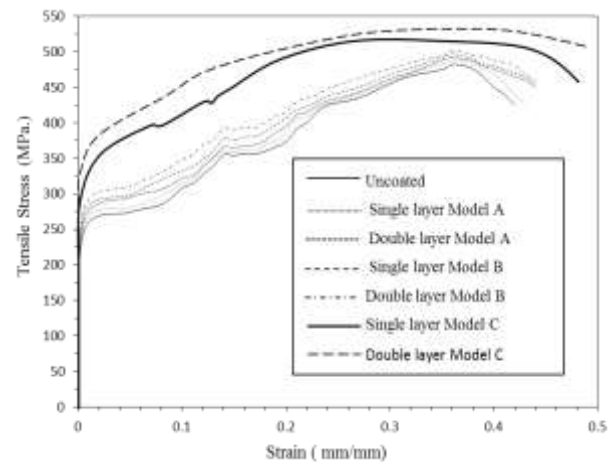


**Figure 6:** Stresses vs. strains of uncoated and coated specimen

**Table 2:** Mechanical properties obtained from the tensile test.

Models	Properties (MPa.)			
	Cases	$S_u$	$S_y$	E
Uncoated	---	484.1	344.3	202.9
Model A	Single layer	488.8	346.2	204.1
	Double layer	492.2	355.3	204.6
Model B	Single layer	497.6	358.4	205.3
	Double layer	501.7	361.5	206.7
Model C	Single layer	525	425	214.2
	Double layer	534	473	216.8

With increasing the temperature, the fragility and suppleness flexibility of epoxy based coatings are increased. The brittleness of epoxy based coating is depending on the flexibility of the chemical components of the basic epoxy and on the type and compositions of the added hardeners. As temperature increases, less cohesive force between the molecules of epoxy and the epoxy group are initiated and leads to decrease the value of the energy needed to break the specimen during test. Model A impact resistance is lower than model B, this attributed to that the high temperature makes model A coatings that consists from amine cured pure epoxy more soft and less toughness compared to model B consists from amine cured Novolac epoxy. The glass-flakes added to the model C are improved the impact resistance by increasing the cohesion between components and giving high rigidity to the coating and making it to have higher impact energy compared to other types.

The impact energy of amines and amine adducts epoxy coating are commonly depending on the temperature. In general the temperature during mixing process of epoxy and base to form the coatings should effect on the impact energy [6].

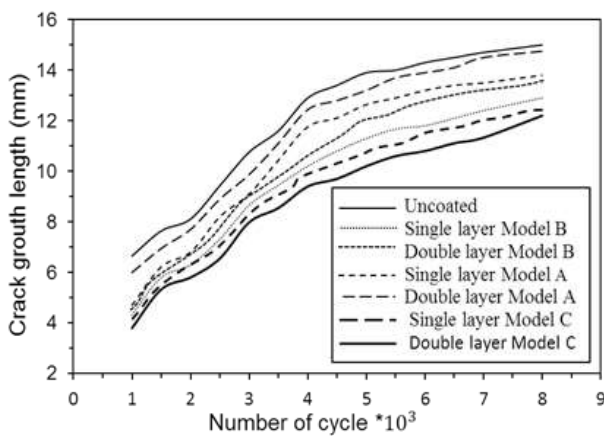
**Table 3:** Charpy impact test results.

Models	Temperature (°C)				
	Cases	15	25	35	45
Uncoated	----	144	141	140	137
Model A	Single layer	147	142	143	141
	Double layer	150	148	145	143
Model B	Single layer	157	156	153	151
	Double layer	161	160	155	152
Model C	Single layer	167	165	160	158
	Double layer	171	169	163	161

### 5.3 Fatigue Test Results

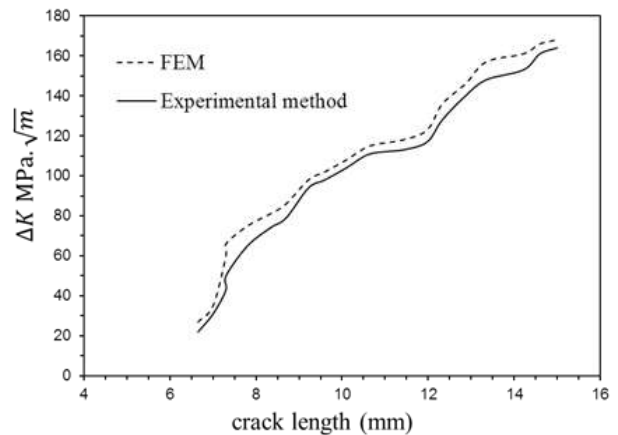
The crack length was measured at each applied cycle during the fatigue crack growth test and the data obtained are plotted as a length of fatigue crack vs. number of applied cycles as shown in Figure 7.

As indicted in Figure7, the uncoated A537 steel and covered by Hampel coatings demonstrated the same propagation behaviors until fatigue fracture occurs. The length of the fatigue crack was quite small in the first cycle of model A. There is a large difference between all coated specimens in a final applied cycle in the fatigue crack length values. This behavior is attributed to the effect of composition of each type of epoxy based coatings. The model C of coatings has greater and better crack extension resistance as well as very high strength compared to the other types of coatings.



**Figure 7:** Crack growth length vs. number of cycle obtained from fatigue test.

By using Ansys V6.7 FEM software program and J-Integral technique, at different cycle loadings, the J-Integral values were calculated for different crack lengths. Five contours are considered for the calculation of the J-Integral values around the crack tip. Using from the J-Integral values, the theoretical maximum stress intensity factors are obtained using Eq.(7). From the measured values of crack length during fatigue crack test for each loading applied on a compact tension specimen, the values of  $K_{max}$ . can be obtained experimentally by Eq.(4). The value of  $\Delta K$  is calculated as the difference  $K_{max}$ .-  $K_{min}$ ., while  $K_{min}$ . = 0 (case no loading applied). Figure 8 shows the comparisons between the values of  $\Delta K$  vs. the length of crack obtained from the fatigue crack test method and FEM. The results obtained from the fatigue crack test method and the results of FEM are in good agreement. Also, the results show that the rate of crack growth is increasing in a non-linear manner with an increase of  $\Delta K$ .



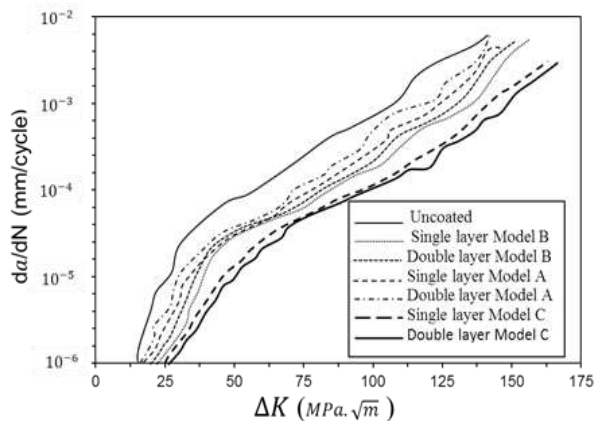
**Figure 8:** Stress intensity factor range vs. crack length obtained from experiment and FEM.

Figure 9 shows the crack growth per load cycle  $da/dN$  vs. stress intensity factor range ( $\Delta K$ ). The  $da/dN$  values are calculated from Figure 8 by means of a tangential method using Eq.(3) based on the number of cycles read after each 2 mm interval. The use of epoxy based coating with A537 steel increases their crack extension resistance compared to uncoated A537 steel.

The relationship between the crack growth rate  $da/dN$  and stress intensity factor range  $\Delta K$  of Figure 9 clearly follows the Paris power law of Eq.(5). The data results of Figure 9 are plotted based on a bi-logarithmic diagram  $\log da/dN$  vs.  $\log \Delta K$  yields the data points aligned on a straight line and then taking slopes of the curves, the value of Paris parameters ( $m$  and  $C$ ) were determined. Table 4 summarizes values of the Paris law parameters for uncoated A537 steel and coated by the three types of models.

Amine-curing Novolac epoxy resin (model B) usually includes multiple epoxy groups such as vinyl groups, alkyl groups, aryl groups... etc. These multiple epoxy

groups have enabled the resin to have high cross-link density, resulting in high crack resistance compared to a mine-curing pure epoxy coats (model A). This model B coating results in higher viscosity due to higher molecular weight, higher number of aromatic ring structures and higher functionality (the number of resin chemical backbone reaction sites). The fatigue cracking behavior of amine epoxy material under mode I is mostly is mostly effected by translation of material from brittle to ductile under effect of applied cyclic loading and this effect on structure of coatings [24].



**Figure 9:** Comparison of fatigue crack growth rate of uncoated and coated A537 steel.

**Table 4.** Paris parameters obtained from Figure 9.

Models	Constants		
	Cases	m	C
Uncoated	----	0.601	$9 * 10^{-6}$
Model A	Single layer	0.65	$5 * 10^{-6}$
	Double layer	0.58	$5.2 * 10^{-6}$
Model B	Single layer	0.53	$5.8 * 10^{-6}$
	Double layer	0.51	$4.4 * 10^{-6}$
Model C	Single layer	0.47	$4.2 * 10^{-6}$
	Double layer	0.46	$3.9 * 10^{-6}$

The higher a resin's functionality, the greater of amine curing Novolac epoxy's crosslink density, this enable their fatigue crack resistance becomes better than that of pure amine curing epoxy. The amine cured pure epoxy coating have lower viscosities compared to model B due to the strong hydrogen bonding through hydroxyl groups that produce less functionality and then fatigue crack resistance. In model C coats, the glass-flake makes the components very cohesive and increases the resistance to crack propagation rates compared to other coating test types. The flake-glass becomes as bridges that are perpendiculars to the crack propagation through the coating and this improves the fatigue crack resistance. The applied cyclic loading enables voids to growth of the epoxy coatings. The growth of voids to cracks effect on

cross linking especially between epoxy coating and steel surface enhanced fracture of coatings [11].

Figure 10 A to E shows the appearance of the fracture surface of uncoated A537 steel and coated specimens by the three models of coatings after rupture throughout the fatigue crack test. Generally, after testing of uncoated A537 steel, no cracking or flaking was observed on all specimen surfaces and the crack extensions were relatively uniform. The single and double layers of model A coating, as observed in Figures 10B and 10C, showed good resistance to crack propagation and no surface crack was observed. The single layer of model A has more surfaces deteriorate than the double layers. In Figures 10D and 10E, for the single and double layer of model B coating, no cracks observes in the surface, but a few spots, defects and some blisters were visible on all of the specimen's surface as a result of testing effect. During the applied loads of fatigue test, the crack will propagate continuously of model A coats, whereas in model B, the cracks will move slowly and simultaneously be accompanied by some plastic deformations at the same time. Figures 10F and 10G, for model C, no damage or spots on the surface of the coat and during fatigue test the crack propagation is linear.

It is found from the shapes of the test specimens rupture surface that during fatigue crack tests there are different methods to generate and spread cracks. The first type is the appearance of a linear crack in the tested specimen. This type is spread linearly through a specimen, resulting in the test specimen creating sharp edges. The second type is generated of cracks due to defects such as bubbles and pores in the thickness of the coating and then spread through the thickness of the material. This type is usually accompanied by small branches of cracks spreading on the surface of the specimen. The third type is the appearance of cracks in test specimen in the form of a slit that extends during the fatigue crack test. The steel inclusions play a role in enhancing the generation of this type of crack.

## 6. Conclusions

The tensile, impact and fatigue testing of three types of epoxy based coatings used as lining for crude oil storage tanks were studied using experimental and finite elements method (FEM). Various conclusions obtained from the analysis of the test results. Based on the Charpy experimental results, it can be clearly seen that at high temperature; the increases of epoxy based coating layers have small effect on the Charpy absorb energy. Also, the results show that there are good agreements between fatigue crack test results and FEM results of stress intensity factor range. Also, the Visual inspection shows stable and linear fatigue crack propagation rate. Amine cured Novolac epoxy have glass-flake more resistance to fatigue crack propagation rate compared to both amine cured Novolac epoxy coats and amine cured pure epoxy coats. Epoxy layers covered the ASTM A537 steel metals increases their fatigue crack resistance regardless of the

type of epoxy based coatings. Double layer of epoxy based coatings improve the fatigue crack resistance by small values compared to the single layer.

### Acknowledgements

The author would express thanks to staff of mechanical Dept. of Technology University of Iraq for their helps and supported the tests.

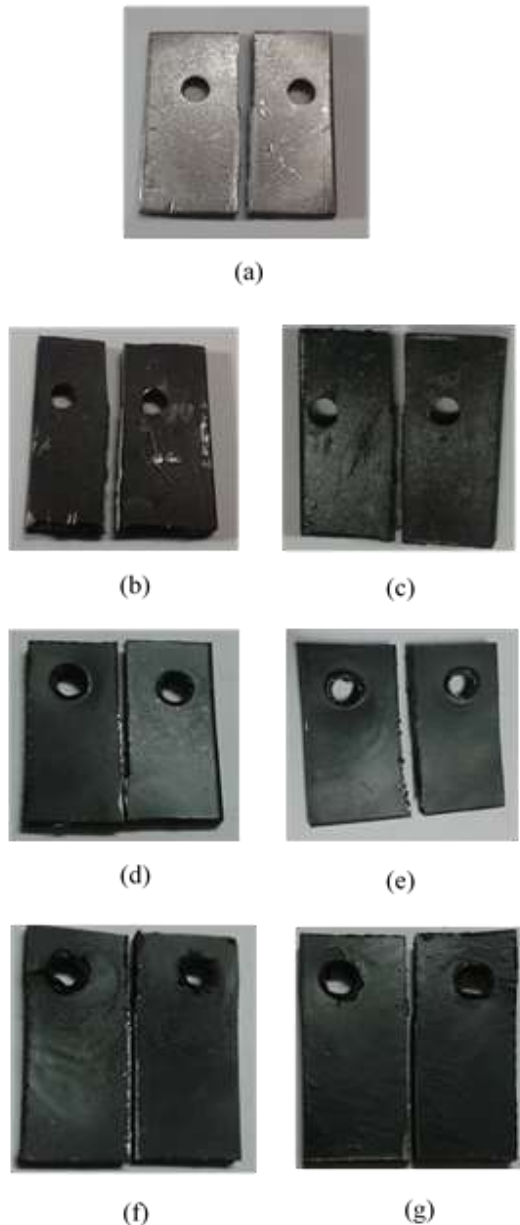


**Figure 10:** Specimen surface after conducted fatigue test.  
 (a) Before coating (b) Single layer model A  
 (c) Double layer model A (d) Single layer model B  
 (e) Double layer model B (f) Single layer model C  
 (g) Double layer model C

### References

- [1] A. A. Mohammad, M. S. El-Sayed, M. Z. Al-Saeed, "Mechanical properties and corrosion behavior of different coatings fabricated by diglycidyl ether of bisphenol-a epoxy resin and aradur r-3282 curing agent", *Int. J. Electrochem. Sci.*, vol.8, pp.8388-8400 2013.
- [2] ASTM E23-72, "Standard test methods for notched bar impact testing of metallic materials", Report of American Society for Testing and Materials, 1982.
- [3] ASTM E647-00, "Standard test method for measurement of fatigue crack growth rates", Report of American Society for Testing and Materials, 1998.
- [4] ASTM E1820-01, "Standard test method for measurement of fracture toughness", American Society for Testing and Materials, USA, 2003.
- [5] A. J. Kinloch, S.H. Lee, and A.C. Taylor "Improving the fracture toughness and the cyclic-fatigue resistance of epoxy-polymer blends", *Polymer*, vol.55,no.24, pp.6325-6334, 2014.
- [6] A. Bahadori, "Essentials of coating, painting, and lining for the oil, gas and petrochemical industries", Ph.D. thesis, Southern Cross University, UK, 2015.
- [7] Andreas K. and Bernd W., Fatigue crack propagation in triblock copolymer toughened epoxy nanocomposites, *Polymer Engineering and Science*, vol.57, no.6, pp.579-587, 2017.
- [8] B. Kim, H. Shin, S. Jung, O. Kraft, Y. Cho and I. Choi, "Crack nucleation during mechanical fatigue in thin metal films on flexible substrates", *Acta Materialia*, vol.61, no.9, pp.347-3481, 2013.
- [9] Bower A. F., "Applied Mechanics of Solids", CRC Press, London 2009.
- [10] C. Kanchanomai and Thammaruechuc A., "Effects of stress ratio on fatigue crack growth of thermoset epoxy resin", *Polymer Degradation and Stability*, 94, pp.1772–1778, 2009.
- [11] D.J. Bray, P. Dittanet, F.J. Guild, A.J. Kinloch, K. Masania, R.A. Pearson AND A.C. Taylor "The modeling of the toughening of epoxy polymers via silica-nano particles: The effects of volume fraction and particle size ", *Polymer*, vol.54, pp.7022-7032, 2013.

- [12] E. R. A. Andres, "Failure pressure and fatigue analysis of the API 12F shop welded flat bottom tanks", M.Sc. Thesis, Purdue University, Indiana, 2016.
- [13] E8/E8M-09, "Standard test methods for tension testing of metallic materials", ASTM International Report, 2000.
- [14] F. Andres, S. Rafael, C. Leiry and R. Alberto, "Crack growth study of dissimilar steels (Stainless-Structural) butt-welded unions under cyclic loads", *Procedia Engineering*, vol.10, pp.1917-1923, 2011.
- [15] G. S. Prinz and A. Nussbaumer, "Fatigue analysis of liquid storage tank shell-to-base connections under multi-axial loading", *Eng. Structures*, vol.40, pp.75-82, 2012.
- [16] G. Nikhil and P. Praveen "An experimental and computational investigation of crack growth initiation in compact tension specimen", *Int. J. of Sci. and Res. Pub.*, vol.2, no.8, pp.1-7, 2012.
- [17] J. W. Sowards, T. S. Weeks and J. D. Mccolskey, "The influence of simulated fuel-grade ethanol on fatigue crack propagation in pipeline and storage tank steels", *Corrosion Science*, 75, pp.415-425 (2013).
- [18] J. Ringsberg and A. Ulfvarson, "On mechanical interaction between steel and coating in stressed and strained exposed locations", *Marine Structures*, vol.11, pp.231-50, 1998.
- [19] K. Holmberg, A. Laukkanen, H. Ronkainen and K. Wallin, "Finite element analysis of coating adhesion failure in pre-existing crack field, Citation *Tribology-Materials*", *Surfaces and Interfaces*, vol.7, no.1, pp.42-51, 2013.
- [20] K. Rege and H. Lemu, "Review of fatigue crack propagation modeling techniques using FEM and XFEM", *Materials Science and Engineering*, vol.276, pp.1-16, 2017.
- [21] [21] K. Sadananda and R. L. Holtz, "Review of fatigue of coatings/substrates", *Conference Proceedings on NATO Advanced Research Workshop on Nanostructured Films and Coatings*, Series 3, vol.78, pp.283-295, Springer Publishers, USA, 2000.
- [22] Linda A. Felton, "Characterization of coating systems", *AAPS Pharm. Sci. Tech.*, vol.8, no.4, pp.1-9 2007.
- [23] M. Wengang and R. Jonas, "Analysis of fatigue crack initiation and propagation in ship structures", 13th International Conference on Fracture, Beijing, China, 2013.
- [24] M. C. Dubourg and A. Chateaumino "Experimental and theoretical investigation of the contact fatigue behaviour of an epoxy polymer under small amplitude sliding micro-motions", *Report of European Structural Integrity Society*, pp.1-16, UK, 2003.
- [25] Philip D. Harvey, *Engineering properties of steels*, Siven-Edition, American Society for Metals, OH, USA, 2003.
- [26] QZ Fang, T. Wang and H. Li, "Tail phenomenon and fatigue crack propagation of PC/ABS alloy", *Polymer Degradation Stab.*, vol.93, no.1, pp.281-90, 2008.
- [27] R. A. Michael, "Fatigue crack initiation and growth in ship structure", M.Sc. Thesis, Denmark Technical University, Denmark, 1998.
- [28] T. Wu, P. E. Irving, D. Ayre, F. Zhao and P. Jackson, "Fatigue cracking behavior of epoxy based marine coating on steel substrate under cyclic tension", *Int. J. of Fatigue*, vol.99, no.1, pp.13-24, 2017.
- [29] W. Tongue, "Investigation of the fracture behavior of epoxy based water ballast tank coatings under static and fatigue loadings, Ph.D. Thesis, Cranfield University, UK, 2015.
- [30] Y. Xu and B. Mellor, "Application of acoustic emission to detect damage mechanisms of particulate filled thermoset polymeric coatings in four points bend tests", *Surface and Coatings Tech. J.*, vol.205, no.5478, 2011.

## تقييم مقاومة الشد، الصدم، ومعدل نمو شق الكلال لطلاء الايبوكسي المستخدم في طلاء خزانات النفط الخام

حيدر هادي جاسم

قسم الهندسة الكيميائية، كلية الهندسة، جامعة البصرة، البصرة، العراق، raidhani73@yahoo.com

نشر في: 30 حزيران 2020

**الخلاصة** – يعتبر ظاهرة الكلال واحد من المسببات الرئيسية للفشل في خزانات النفط الخام. من أجل تقييم سلامة معدن المستخدم في الخزانات والطلاء المستخدم، نحتاج الى اختبار وتقييم فشل الكلال. في هذا البحث، تم اختبار ودراسة مقاومة الشد، الصدم والكلال لثلاثة انواع من طلاءات الايبوكسي (نقي، فينول نوفالاك، مقوى بقطع الزجاج) باستخدام الطرق العملية وطريقة العناصر المحددة. اجريت التجارب العملية وحسابات طريقة العناصر المحددة على العينات غير المطلية للصلب الكربوني نوع ASTM A537 C1 والمطلية لحالتين طلاء بطبقة واحدة والطلاء بطبقتين. بينت النتائج ان الطلاء بشكل عام يحسن الخواص الميكانيكية ويزيد المقاومة ضد نمو شق الكلال. كذلك وجد ان نمو شق الكلال يتأثر بتركيب مادة طلاء الايبوكسي وان الطلاء المقوى بقطع الزجاج ابدى مقاومة اكبر للكلال مقارنة بالطلاء الايبوكسي النقي او الفينول نوفالاك. الفحوصات المايكروسكوبية بينت ان انتشار الشق الكلال يكون منتظم ومستقر ومن النوع الخطي.

**الكلمات الرئيسية** – المجموعة الفعالة، طلاء الايبوكسي، شقوق الكلال، تكامل جي، قطع الزجاج.